

**Structural Analysis to Qualify Hanford Double-Shell Tanks for Increased Waste Storage - 21150**

Kenneth I. Johnson\*, John E. Deibler\*, Naveen K. Karri\*,

F. George Abatt\*\*, Kenneth L. Stoops\*\*, Larry J. Julyk\*\*,

\*Pacific Northwest National Laboratory, Richland, Washington 99352

\*\* Becht, Richland, Washington 99352

**ABSTRACT**

Ensuring adequate waste storage volume is critical to the success of the U.S. Department of Energy's mission to retrieve, treat, and dispose of the radioactive waste in the Hanford tank farms. Using more of the available waste storage volume in the existing double-shell tanks is an attractive option compared to constructing new tanks. In 2008, detailed structural analysis of the AP tank design, the newest double-shell tank farm, provided the justification to increase the allowable waste level in the AP tanks. A similar analysis was recently completed for the next-newest double-shell tanks in the AN and AW tank farms using updated analysis methods and design response spectra based on the most recent (2014) probabilistic seismic hazard analysis. Detailed finite element models of the reinforced concrete tank structure and the surrounding soil were developed for the analysis of both the thermal and operating loads and the seismic loads. The thermal-structural model simulates the operating history to include the effects of storing waste at temperatures up to 66°C on thermal stresses and the stiffness and strength properties of the concrete. The seismic analysis evaluated design response spectra for both high-frequency and low-frequency earthquake shaking. The high-frequency spectra were developed from separate hazard curves for earthquakes of magnitudes less than eight, which are principally local crustal earthquakes. The low-frequency spectra were developed for earthquakes of magnitudes eight and greater, which may result from distant earthquakes along the Cascadia subduction zone. The seismic accelerations generate loads in the reinforced concrete structure, but also waste sloshing loads in the steel primary tank. The modeling techniques used in the sloshing analysis are highlighted, and this paper summarizes the engineering analysis methods used to evaluate the structural integrity of the reinforced concrete tank shell, the steel primary and secondary tank liners, and the anchor bolts that attach the primary tank to the reinforced concrete dome. The analysis concludes that the AN and AW tanks will continue to satisfy the governing structural codes in their current condition with the maximum waste level increased from 10.7 to 11.7 meters.

**INTRODUCTION**

Beginning in 1943, underground waste storage tanks were constructed at the Hanford Site to contain the waste generated by the chemical processes used to separate nuclear materials. Between 1943 and 1965, 149 single-shell tanks were constructed. After 1965, the newer waste tank designs included double-shell containment systems that provide a second barrier to prevent waste from leaking into the soil beneath the tanks. These double-shell tanks (DSTs) consist of an inner steel primary tank with a secondary steel liner covered by a reinforced concrete shell. TABLE I lists the chronology of the 28 DSTs that were constructed between 1968 and 1986. The DSTs have a 22.9-meter (75-foot) inside diameter and a storage capacity of 4,400 cubic meters (1.16 million gallons) at the maximum specified waste height of 10.7 meters (422 inches). However, there is approximately 1 meter (38 inches) of additional wall height that could be used to increase the waste capacity to approximately 4,800 cubic meters (1.27 million gallons). To allow filling the tanks to the higher level, it must be shown that the tanks have sufficient structural strength to support the additional waste under static plus seismic loads.

TABLE I. The Chronology of Double-Shell Tanks Constructed at the Hanford Site

| Tank Farm | Number of Tanks | Construction Period | Initial Operation | Service Life | Current Age |
|-----------|-----------------|---------------------|-------------------|--------------|-------------|
| 241-AY    | 2               | 1968 – 1970         | 1971              | 40           | 49          |
| 241-AZ    | 2               | 1970 – 1974         | 1976              | 20           | 44          |
| 241-SY    | 3               | 1974 – 1976         | 1977              | 50           | 43          |
| 241-AW    | 6               | 1976 – 1979         | 1980              | 50           | 40          |
| 241-AN    | 7               | 1977 – 1980         | 1981              | 50           | 39          |
| 241-AP    | 8               | 1982 – 1986         | 1986              | 50           | 34          |
| Total     | 28              |                     |                   |              |             |

A detailed structural analysis completed in 2008 showed that the DSTs in the newest AP tank farm had adequate structural margin to increase the waste level from 10.7 to 11.7 meters [1]. This paper highlights the methods used in a recent analysis to justify increasing the waste level to 11.7 meters in the AN and AW tanks [2]. Increasing the allowable waste level by 1 meter in each of the 13 AN and AW DSTs would provide 5,150 cubic meters of additional storage capacity, equal to more than one full DST. This is a significant increase in storage volume that would allow more flexibility in waste storage and retrieval operations during the Hanford waste treatment mission.

Of the different tank designs used in the six DST farms, the AN and AW designs are essentially identical and they are most similar to the AP tanks. The AP, AN, and AW tanks are the newest DSTs and were designed with higher strength concrete, better primary tank steel, and thicker primary tank walls than the AY, AZ, and SY tanks. TABLE I shows that the AN and AW tanks also have 10 to 11 years remaining within their design service lives. These characteristics make the AN and AW tanks the best candidates for increasing the allowable waste level.

### THE THERMAL AND OPERATING LOADS ANALYSIS

Structural analyses evaluated the static thermal and operating loads that the AN and AW tanks have experienced during their years of waste storage as well as the design basis earthquake loads that must be considered during the remaining operating lives of the tanks. PNNL performed the static thermal and operating loads analysis (TOLA) and Becht was subcontracted to perform the seismic analysis. Both the TOLA and seismic models were developed using the ANSYS® finite element software.

The TOLA model shown in Fig. 1(a) includes the soil surrounding the tank, the reinforced concrete tank structure, the inner primary tank and secondary liner, and the contact conditions between each of these structural features. Fig. 1(b) shows the locations around the tank cross-section where force and moment loads were extracted to analyze the reinforced concrete. The tank section demands are evaluated in both the hoop and meridional directions corresponding to the orientation of the steel reinforcements. The reinforced concrete was modeled using the ANSYS® SOLID65 concrete elements, which are capable of simulating the expected cracking behavior of reinforced concrete under load. The concrete elements can also be defined to include the fractional area of steel reinforcing bars in both the meridional and hoop directions. Fig. 2(a) and (b) show where the reinforcements are located in the tank dome, haunch, wall, and footing that correspond to the reinforcements specified in the design drawings. The steel primary tank and secondary liner were modeled using ANSYS® SHELL181 elements.

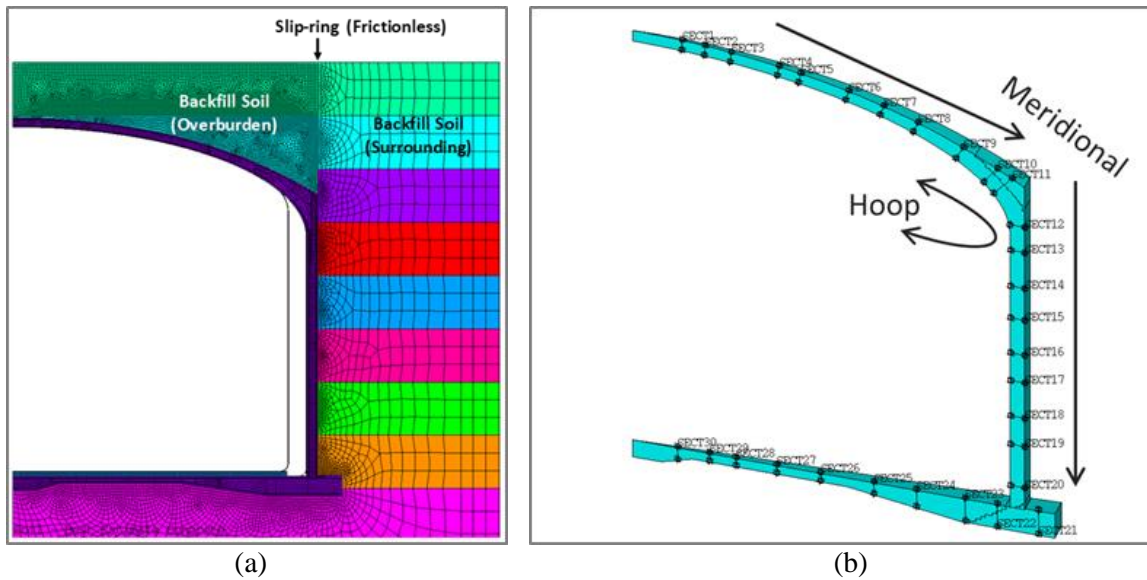


Fig. 1. TOLA model showing (a) the tank and surrounding soil and (b) the tank sections where force and moment demands are extracted from the TOLA and seismic models.

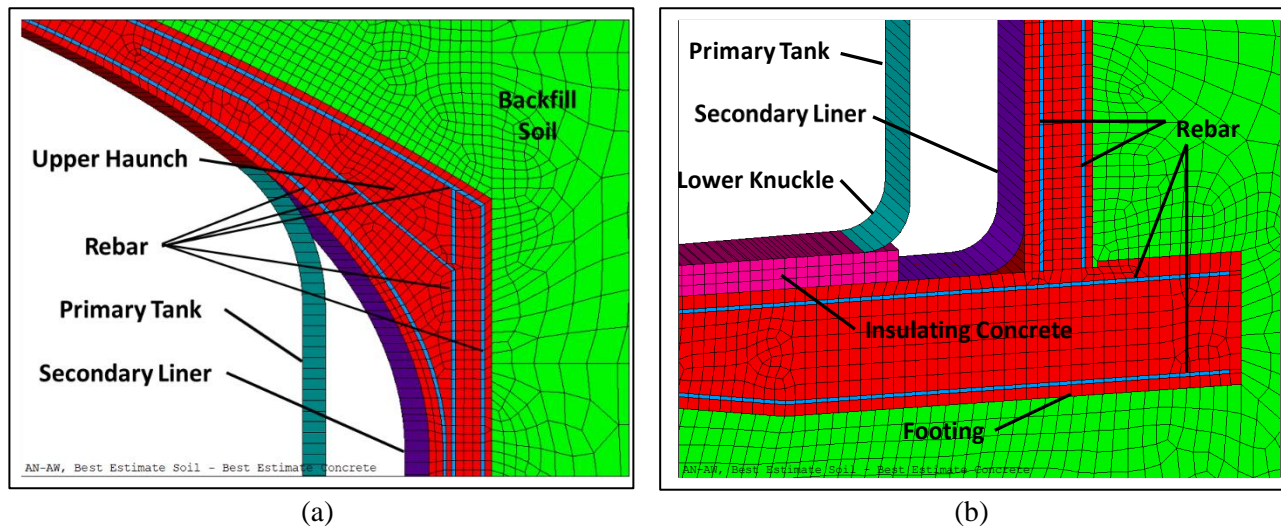


Fig. 2. Closeup of model details in the tank cross-sections in (a) the upper haunch and (b) the lower knuckle.

The soil was modeled using SOLID185 elements with the extended Drucker-Prager, pressure-dependent yield criterion. While the soil in the TOLA model does yield and redistribute the pressure on the tank as gravity is applied, the resulting soil pressures do not match the at-rest pressure distribution that is expected from the soil layering and compaction process used to backfill the soil around and above the tanks. The best estimate, at-rest soil pressure distribution is  $\rho gh$  (density  $\times$  gravity  $\times$  soil depth) on the dome surface and  $1/2 \rho gh$  on the vertical tank wall. To enforce these soil pressures, an interactive algorithm was developed to adjust the local soil contact offsets in the sidewall and dome until the at-rest pressure distribution was achieved during the initial application of gravity. The algorithm iterates automatically until the root-mean square error between the calculated and at-rest pressures is reduced to a

specified tolerance. Fig. 1(a) shows the slip ring that was also included in the soil at the outside radius of the dome to prevent the soil from artificially bridging over the dome.

The thermal analysis was performed using an axisymmetric model that is a subset of the structural model. The structural elements were changed to thermal elements and a series for transient thermal load steps were analyzed to simulate the thermal operating history of the tanks. The thermal cycle used in the analysis was an aggressive 1-year-long fill and drain cycle that applied the maximum heat-up and cool-down rates from the tank specifications. Although the AN and AW DSTs have a design life of 50 years, an extended 60-year operating history was simulated to include the expected service life required for waste retrieval and closure.

The thermal analysis began with 5 yearly thermal cycles that account for thermal ratcheting and shake-down of the loads in the tank structure. When the tank reached the steady state peak temperatures in the first year, the thermally degraded concrete stiffness properties were applied to the model. Additional thermal cycles intermixed with long hold times at the steady-state peak waste temperature (66°C) were simulated to capture any additional ratcheting effect that long-term creep may have had on the cracking of the concrete and subsequent load redistribution. The waste level was then increased from 10.7 to 11.7 meters after the year 2017 when this project initiated. The tank evaluations were conducted in the 60<sup>th</sup> year of the simulated operating history.

The anchor bolts that attach the steel primary tank to the reinforced concrete dome were modeled with spring elements (COMBIN40) that have a shear secant stiffness determined from a detailed finite element analysis of the welded stud and threaded anchor system [1]. Fig. 3(a) shows the L-bolt threaded anchors in an AW tank construction photo and Fig. 3(b) shows the finite element model of the deformed anchor stud. The analysis simulated plastic deformation of the welded stud and anchor plus crushing of the surrounding concrete. The results show a non-linear shear force versus displacement response, where most of the shear deformation occurs in the cylindrical tapped stud. The secant stiffness (the linear slope from zero to a point on the force/displacement curve) decreases as the shear displacement increases with more and more deformation in the welded stud and crushing of the surrounding concrete. Consequently, the geometry of the remote end buried in concrete (J-bolt, L-bolt, or headed stud) does not affect the shear response of the anchor bolt.

The model results were correlated with the manufacturer's load-displacement data to establish the lower bound shear secant stiffness used in the analysis. The uniform, elastic secant stiffness used to model the anchor bolts corresponds to the maximum shear displacement at the outermost ring of anchors bolts. Using this secant stiffness for the inboard anchors is conservative because it overestimates the shear forces in the outer rings of anchor bolts. The secant stiffness would be greater for the anchors closer to the dome center, where the shear displacements are smaller. The anchor stiffness in the axisymmetric models was defined as a function of radius from the dome center to represent the 0.6-meter anchor spacing around the dome.

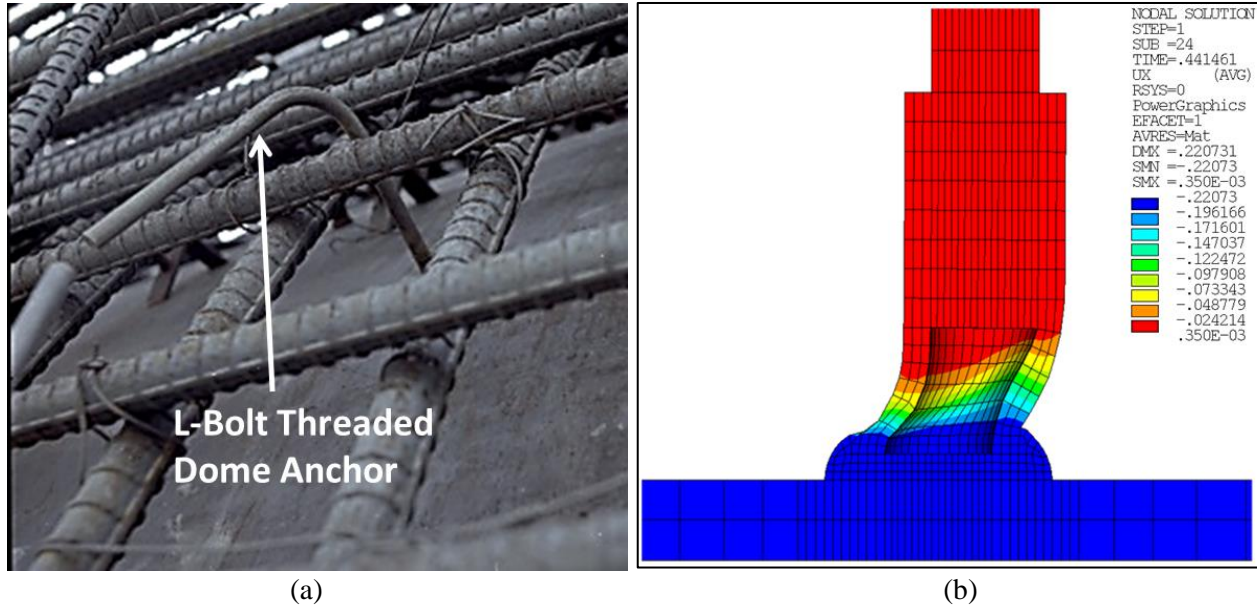


Fig. 3. (a) AW tank construction photo showing L-bolt dome anchors and (b) anchor stud shear deformation model used to calculate the anchor shear stiffness used in the model (concrete surrounding the anchor stud not shown for clarity).

### THE SEISMIC LOADS ANALYSIS

Since 2004, a series of seismic analyses of record have been performed on the Hanford DSTs. These analyses are documented in [1, 3-4], among others. In contrast to earlier analyses, several notable changes are incorporated in the seismic analysis supporting the increased liquid level in the AN and AW tanks. This section discusses three of these changes and the resulting effect on the seismic analysis: (1) use of an updated probabilistic seismic hazard analysis (PSHA) to develop the ground motions, (2) separation of the ground motions into low-frequency and high-frequency records, and (3) improved modeling of the liquid waste sloshing.

The seismic input for previous DST analyses was developed based on a 1996 Hanford PSHA. The ground motions for this project are based on the most recent PSHA, issued in 2014 [5]. The process to develop the ground motions was changed somewhat to follow the provisions of ASCE/SEI 7-10 [6] more closely.

Because this analysis supports increasing the waste level in the AN/AW tanks, sloshing of the waste is a focus of the seismic analysis. This motivated the development of separate, low-frequency spectra to supplement the high-frequency spectra to better capture the low-frequency convective response of the liquid waste.

Fig. 4 compares the design response spectra (DRS) used for the previous analyses cited above with the DRS used for this project. Two observations are clear. First, the updated spectral accelerations are significantly lower in magnitude compared to the previously used spectra above approximately 1 Hz. Second, the low-frequency spectral accelerations are higher in magnitude than the previously used spectra below approximately 1 Hz.

The high-frequency DRS provide seismic excitation across the range of frequencies at and above those at which structures typically respond (1 to 30 Hz). The low-frequency DRS provide greater excitation in the frequency range of 0.1 to 1 Hz – a range that includes the convective (sloshing) response modes of the

waste. The low-frequency excitation is dominated by a more distant seismic source in the Cascadia subduction zone.

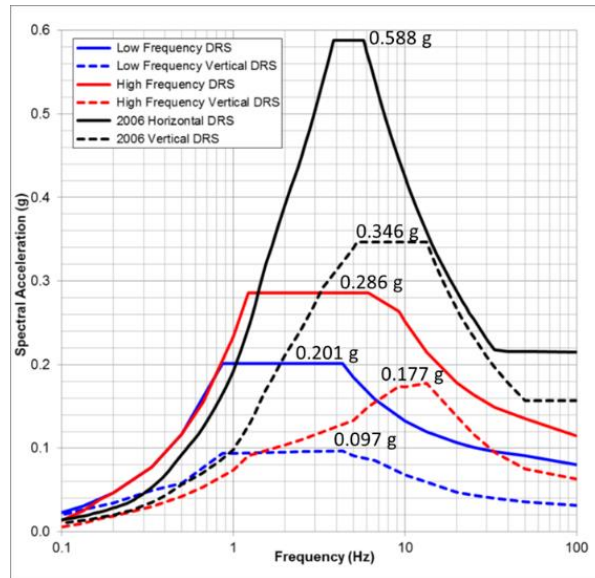


Fig. 4. Comparison of design response spectra.

Due to the long period response of the convective modes, longer runs are required to allow the low-frequency convective response to fully develop. However, if sloshing of the waste is not a concern, or if it has little influence on the structural demands, it may be desirable to perform shorter runs using only the high-frequency input. Development of separate low- and high-frequency ground motions allows this flexibility in future analyses. Based on the above observations, it is expected that the seismic response of the tank/liquid system will be reduced relative to the previous analysis with the exception of convective fluid-structure interaction effects, which tend to be localized near the waste free surface.

Previous analyses of record of the DSTs used the ANSYS® SOLID45 element, which is a 3D linear elastic structural solid element, to simulate the liquid waste. In this approach, the SOLID45 elements were assigned a low shear modulus and a Poisson’s ratio of slightly less than 0.5 to better simulate an incompressible liquid. Although this approach was effective in capturing the impulsive response of the tank/waste system, the overall reactions, and the loads caused by the convective response, some information was lost in capturing the details of the local convective response.

In the current analysis, ANSYS® FLUID80 element was selected to simulate the tank waste. The FLUID80 element is a displacement-based incompressible fluid element that is well-suited for calculating hydrostatic pressures and fluid/solid interactions. The element includes special surface options to enable free surface effects, such as sloshing in a transient analysis. The FLUID80 element is a “legacy” element. While newer ANSYS fluid elements exist, experience has shown they are not as well-suited for this particular application.

The use of FLUID80 elements can be technically challenging as it is prone to instability and has a high sensitivity to mesh distortion, which can occur in elements closest to the fluid-structure interface. Excessive element distortion can result in spurious and unreasonable displacements. The stability of FLUID80 is also sensitive to the solution options selected. Consequently, the use of FLUID80 requires benchmarking to assure that the model is functioning as expected. The benchmarking is discussed below.

FLUID80 elements were used over the entire free surface, down to the full depth of the waste. A thin annulus of SOLID45 elements is used along the tank wall beyond the radius of the free surface. This region contains the 3D curved geometry at the dome haunch and lower knuckle. SOLID45 elements are used there because the FLUID80 element was found to be too unstable to use the triangular prismatic elements needed for the mesh. This region does not initially contain a free surface, so the elements need only be capable of transmitting the hydrostatic and impulsive loads, a function the SOLID45 element performs well. However, this means that when the free surface elevation at the outer radius decreases during the seismic event, the outer radius will follow the SOLID45 annulus, not the primary tank. The difference in the effective radius of the waste (11 meters vs. 11.4 meters) has a negligible effect on the results.

Radial couples are applied between the FLUID80 and SOLID45 elements, which allows the FLUID80 to slosh freely in the vertical direction and to transmit the fluid pressure demand outward to the primary tank walls. The SOLID45 waste elements are meshed such that there are common (merged) nodes with the primary tank. The FLUID80 and SOLID45 elements are shown in Fig. 5.

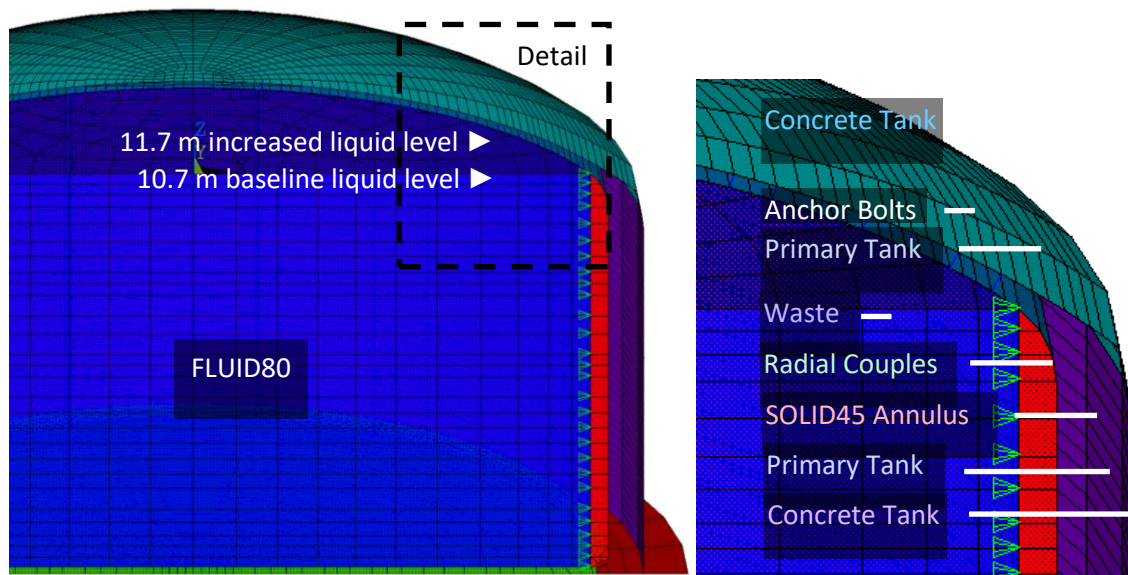


Fig. 5. Model plot of tank and waste with detail at waste fill line.

The interface between the waste free-surface and the primary tank dome uses a combination of ANSYS® TARGE170 and CONTA173 elements. Unlike all other interfaces in the model, this frictionless interface is initially open under deadweight loading, and only closes because of fluid sloshing against the dome during the seismic transient. The contact stiffness of this interface is reduced by a factor of 1,000 from the default value to improve solution stability.

Initial approaches used a very low stiffness shell layer overlaid on the free surface to improve solution stability, but while this approach did improve stability, it was rejected due to the undesirable side effect of artificially reducing the convective response.

Verification of the fluid response was performed using a simplified sub-model, which was modified to match the assumptions in the theoretical response calculations. Calculations for the theoretical fluid response are based on equations provided in Chapter 4 of [7]. The theoretical response is applicable to a bottom-supported free-standing cylindrical tank with an open top. The contained liquid is assumed to be

incompressible and inviscid. Critical damping of the water-like waste is set to 0.5% following Table 6-2 of ASCE 4-16 [8] for the convective response of the liquid.

Comparison to the theoretical response demonstrates the sub-model’s ability to simulate fluid behavior, particularly for sloshing. The fluid response in the sub-model with an open top shows the dominant first convective mode, where the fluid rises at one side of the tank and falls at the opposite side. The model’s maximum slosh height, frequency, and hydrodynamic force are a good match to the values predicted by the analytical solution. Fig. 6 shows the waste slosh height history of the sub-model with low-frequency input from the best estimate soil and best estimate concrete full DST model.

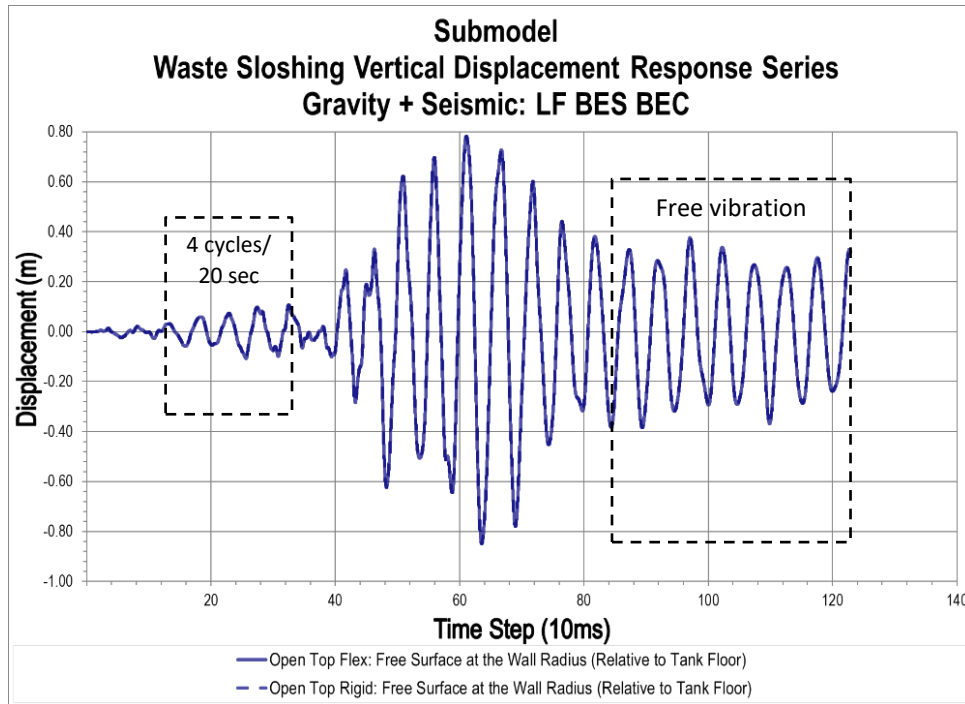


Fig. 6. Waste slosh height over time – benchmarking sub-model.

The sub-model benchmarking provides confidence that the DST model is working as intended. However, the presence of the tank dome is a major difference between the sub-model and the DST model, and this affects the solution. The tank dome constrains the upward movement of the waste, although the amplitude of the downward movement could approach the theoretical slosh height for an open top tank. In a domed tank, the maximum upward movement is constrained horizontally and vertically. The downward movement is unconstrained vertically, although the constraints on the opposite (rising) side can be expected to slightly reduce the amplitude as the effective free surface width is reduced in the dome.

The fluid’s interaction with the tank dome in the DST model causes surface wave reflections at a shorter radius than the tank wall, giving rise to additional waves at shorter periods. These reflections constructively superimpose over time, to the point where they dominate over the first convective mode response. The reported maximum wave amplitude represents both the fundamental convective response along with shorter period superimposed waves. In contrast, the free surface in the benchmark model remains generally planar because the first convective mode dominates. Test runs performed with the viscosity of water showed that the 0.5% critical damping used in this analysis reduces these additional waves significantly relative to using zero damping in the solution, even with the viscosity present.

Fig. 7 shows an example of the strong convective response of waste sloshing in the DST model. This profile occurred 63 seconds into the low-frequency seismic event. The free surface shows superimposed out-of-phase waves caused by reflections off the edge of the dome.

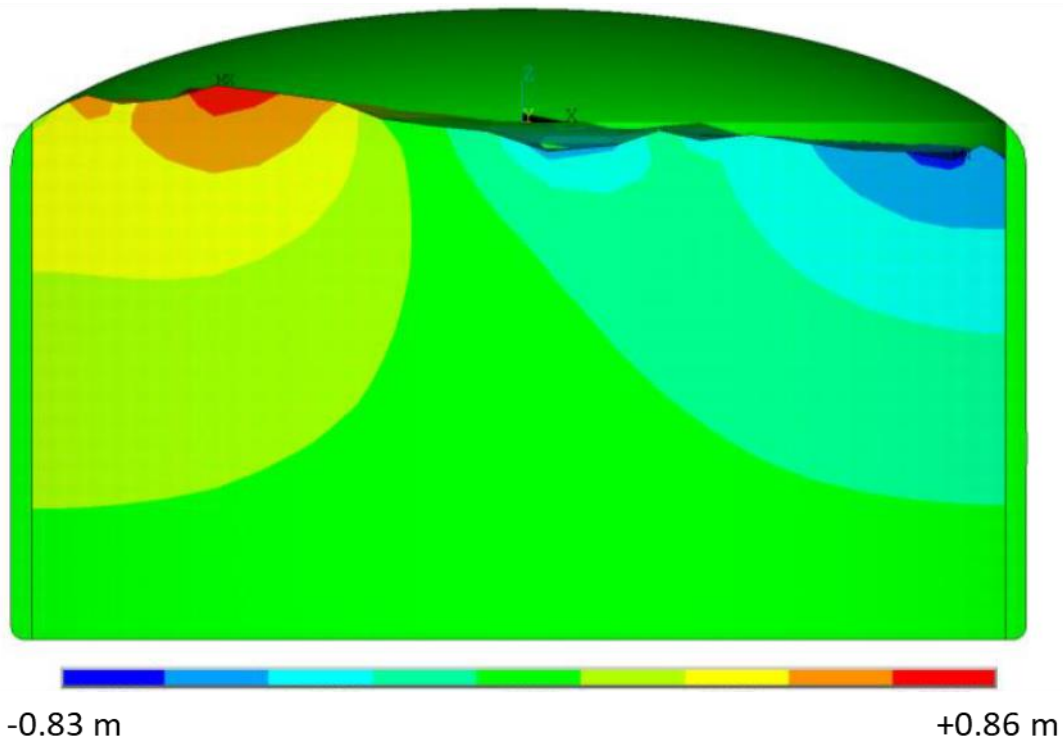


Fig. 7. Waste slosh height profile at 63 seconds into the low-frequency seismic event.

The overall effect of the changes in this seismic analysis are 1) lower seismic demand due to lower seismic input accelerations, except at frequencies below approximately 1 Hz, 2) better fidelity in the local convective waste sloshing response due to both a change in the elements representing the liquid waste and separately developed low-frequency seismic input, and 3) additional flexibility for future analyses of liquid filled and empty tanks with separate high- and low-frequency design response spectra.

## ANALYSIS RESULTS

The AN-AW level rise analysis of record evaluated many aspects of the tank structural integrity.

The reinforced concrete tank shell was evaluated to the force-based design criteria of the ACI 349 code for nuclear safety-related concrete structures [9]. Several static and seismic load combinations were evaluated and the force-based section demands were found to be less than the ACI section capacities. A limit load analysis was also performed that showed the calculated collapse loads were more than three times the current soil and equipment loads above the tank domes. Finally, a concrete shell buckling analysis was performed that further confirmed the structural stability of the tanks under load.

The steel primary tank was evaluated to the stress requirements of the ASME Boiler and Pressure Vessel (B&PV) Code [10]. The primary tank stress intensities from TOLA loads plus seismic waste sloshing loads were only 53% of the ASME allowable stress intensities. Stress corrosion cracking of the steel primary tank wall was also determined to be very unlikely based on the recent evaluations of the AY-102 tank leak and fracture mechanics analysis. The membrane and bending stresses applied to an assumed

maximum undetectable initial surface flaw were not high enough to initiate stress corrosion cracking. The primary tank buckling analysis also showed that the operational vacuum limit placed on the primary tank ventilation system is lower than the vacuum limit calculated from large-displacement, finite element buckling analysis.

The steel secondary liner of the AN-AW tanks was evaluated to the strain limits for steel backed by concrete specified in the ASME B&PV code [11]. The secondary liner strains were less than 20% of the ASME allowable strains.

Finally, the anchor bolts connecting the primary tank to the concrete dome were evaluated using a limit load criteria developed from elastic-plastic finite element analysis of the anchor stud embedded in concrete and correlated with the anchor manufacturer's load-deflection test data. At the maximum waste temperature condition, the maximum shear load in the outer ring of anchors was only 63% of the anchor capacity.

## CONCLUSIONS

A detailed structural analysis was conducted to determine if the structural code standards that govern operation of the AN and AW DSTs at Hanford are satisfied with the waste level increased from 10.7 to 11.7 meters. The analysis evaluated both TOLA and seismic loads, which were combined to evaluate multiple structural criteria that establish the allowable loads on the DSTs. Both low-frequency and high-frequency earthquake spectra were analyzed to capture the low-frequency sloshing in the primary tank and the higher frequency response of the reinforced concrete outer shell. The seismic spectra were developed from the most recent PSHA of the Hanford Site [5].

Many aspects of the DST tank structure were evaluated, including forces and moments in the reinforced concrete tanks, stresses in the primary tank, strains in the secondary liner backed by concrete, and forces in the anchor bolts connecting the primary tank to the reinforced concrete dome. Buckling and limit load analyses were also conducted to confirm the structural stability of the tanks and the large margin between the operating loads and the maximum loads at the onset of dome collapse. The primary tank was also checked to ensure that increasing the waste level would not increase the likelihood of stress corrosion cracking in the primary tank.

The conclusion from all of these analyses was that the structural capacity of AN and AW tanks exceeds the structural demands placed on the tanks. Therefore, it was determined that adequate structural margin remains in the AN and AW tanks with the waste level increased from 10.7 to 11.7 meters.

## REFERENCES

1. J. E. DEIBLER, K. I. JOHNSON, S. P. PILLI, M. W. RINKER, F. G. ABATT, and N. K. KARRI, *Hanford Double-Shell Tank Thermal and Seismic Project – Increased Liquid Level Analysis for 241-AP Tank Farms*, RPP-RPT-32237, Rev. 1, Pacific Northwest National Laboratory, Richland, WA (2008a).
2. K. I. JOHNSON, J. E. DEIBLER, N. K. KARRI, F. G. ABATT, K. L. STOOPS, and L. J. JULYK, *AN-AW Level Rise Structural Integrity Analysis of Record*, RPP-RPT-60175, Rev. 0; PNNL-30097, Pacific Northwest National Laboratory, Richland, WA (2021).
3. J. E. DEIBLER, M. W. RINKER, K. I. JOHNSON, F. G. ABATT, N. K. KARRI, S. P. PILLI, and K. L. STOOPS, *Hanford Double-Shell Tank Thermal and Seismic Project – Summary of Combined Thermal and Operating Loads With Seismic Analysis*, RPP-RPT-28968, Rev. 1; PNNL-15721, Pacific Northwest National Laboratory, Richland, WA (2008b).
4. M. W. RINKER and F. G. ABATT, *Hanford Double Shell Tank Thermal and Seismic Project – Dytran® Benchmark Analysis of Seismically Induced Fluid-Structure Interaction in a Hanford*

*Double Shell Primary Tank*, RPP-RPT-28963, Rev. 1; PNNL-15704, Pacific Northwest National Laboratory, Richland, WA (2008).

5. PACIFIC NORTHWEST NATIONAL LABORATORY, *Hanford Sitewide Probabilistic Seismic Hazard Analysis*, PNNL-23361, Richland, WA (2014).
6. AMERICAN SOCIETY OF CIVIL ENGINEERS, *Minimum Design Loads for Buildings and Other Structures*, ASCE/SEI 7-10, Reston, VA (2013).
7. BROOKHAVEN NATIONAL LABORATORY, *Seismic Design and Evaluation Guidelines for the Department of Energy High Level Waste Storage Tanks and Appurtenances*, Report No. 52361, Engineering Research and Applications Division, Department of Advanced Technology, Brookhaven National Laboratory, Associated Universities, Inc., Upton, NY (1995).
8. AMERICAN SOCIETY OF CIVIL ENGINEERS, *Seismic Analysis of Safety-Related Nuclear Structures*, ASCE 4-16, Reston, VA (2017).
9. AMERICAN CONCRETE INSTITUTE, *Code Requirements for Nuclear Safety-Related Concrete Structures (ACI 349-06) and Commentary*, Farmington Hills, MI (2007).
10. AMERICAN SOCIETY OF MECHANICAL ENGINEERS, *Boiler and Pressure Vessel Code*, Section III, Division 1, Subsection NC, Class 2 Components - Rules for Construction of Nuclear Plant Components, New York, NY (1992a).
11. AMERICAN SOCIETY OF MECHANICAL ENGINEERS, *Boiler and Pressure Vessel Code*, Section III, Division 2, Subsection CC, Concrete Containments (Prestressed or Reinforced), New York, NY (1992b).

#### **ACKNOWLEDGEMENTS**

The authors would like to acknowledge the management and engineering support of Washington River Protection Solutions and the funding provided on behalf of the U.S. Department of Energy, Office of River Protection to perform these structural analyses.

#### **TRADEMARK DISCLAIMER**

Reference herein to any specific commercial product, process, or service by trade name, trademark, manufacturer, or otherwise, does not necessarily constitute or imply its endorsement, recommendation, or favoring by the United States Government or any agency thereof or its contractors or subcontractors.